processes

MDPI

Article

Enhancing Astaxanthin Biosynthesis by *Rhodosporidium toruloides* Mutants and Optimization of Medium Compositions Using Response Surface Methodology

Tuyet Nhung Tran [1,2], Dai-Hung Ngo [3], Quoc Tuan Tran [1,2], Hoang Chinh Nguyen [4,5,*], Chia-Hung Su [5] and Dai-Nghiep Ngo [1,2,*]

1 Faculty of Biology and Biotechnology, University of Science, Ho Chi Minh City 700000, Vietnam; tranthituyetnhung@tdtu.edu.vn (T.N.T.); tqtuan@hcmus.edu.vn (Q.T.T.)
2 Vietnam National University Ho Chi Minh City, Ho Chi Minh City 700000, Vietnam
3 Faculty of Natural Sciences, Thu Dau Mot University, Binh Duong 590000, Vietnam; hungnd@tdmu.edu.vn
4 Graduate Institute of Applied Science and Technology, National Taiwan University of Science and Technology, Taipei 10607, Taiwan
5 Graduate School of Biochemical Engineering, Ming Chi University of Technology, New Taipei City 24301, Taiwan; chsu@mail.mcut.edu.tw
* Correspondence: nguyenhoangchinh@tdtu.edu.vn (H.C.N.); ndnghiep@hcmus.edu.vn (D.-N.N.)

Received: 26 March 2020; Accepted: 21 April 2020; Published: 24 April 2020

Abstract: Astaxanthin is a valuable carotenoid, which has been approved as a food coloring by the US Food and Drug Administration and is considered as a food dye by the European Union (European Commission). This work aimed to attain *Rhodosporidium toruloides* mutants for enhanced astaxanthin accumulation using ultraviolet (UV) and gamma irradiation mutagenesis. Gamma irradiation was shown to be more efficient than UV for producing astaxanthin-overproducer. Among the screened mutants, G17, a gamma-induced mutant, exhibited the highest astaxanthin production, which was significantly higher than that of the wild strain. Response surface methodology was then applied to optimize the medium compositions for maximizing astaxanthin production by the mutant G17. The optimal medium compositions for the cultivation of G17 were determined as a peptone concentration of 19.75 g/L, malt extract concentration of 13.56 g/L, and glucose concentration of 19.92 g/L, with the maximum astaxanthin yield of 3021.34 µg/L ± 16.49 µg/L. This study suggests that the *R. toruloides* mutant (G17) is a potential candidate for astaxanthin production.

Keywords: astaxanthin accumulation; mutant; medium composition; *Rhodosporidium toruloides*; optimization

1. Introduction

Astaxanthin (3,3′-dihydroxy-β-carotene-4,4′-dione) is a keto-carotenoid with extensive use as a feed supplement in aquaculture industry due to its contributions to the attractive coloration, growth, and survival of marine animals such as shrimps, salmon, and trout [1,2]. Astaxanthin has been approved as a color additive for specific uses in fish and animal foods by the Food and Drug Administration (FDA, USA) [3]. The European Union also considers astaxanthin as a food dye within the E number system (E161j) [3]. Furthermore, astaxanthin has a strong antioxidant activity and reveals a potential therapeutic agent against various diseases such as cardiovascular disease, skin-related illness, atherosclerotic, and cancer [4,5]. Therefore, astaxanthin has various applications in pharmaceutical, nutraceutical, and cosmetic industries [3,6]. Because of such benefits, there is an

increasing demand for astaxanthin, which consequently requires an efficient and safe approach for astaxanthin production.

Astaxanthin is commonly synthesized by using a chemical process [6]. Although this process can produce astaxanthin in large quantities, it has a negative effect on environment [7]. Remarkably, concerns remain about the food safety and biological function of the synthetic astaxanthin [8,9]. To prevent these obstacles, using microorganisms for natural astaxanthin production has increasingly gained considerable interest as microorganisms can produce astaxanthin through their biosynthesis pathway [10,11]. Bacteria (e.g., *Brevibacterium* sp. [12] and *Escherichia coli* [13]) and green microalgae (e.g., *Chromochloris zofingiensis* (formerly *Chlorella zofingiensis*) [14] and *Haematococcus lacustris* (formerly *Haematococcus pluvialis*) [15]) have been mainly studied for astaxanthin synthesis. Among them, *H. lacustris* is a potential source of astaxanthin because of its high content of astaxanthin [16,17]. Nevertheless, the use of *H. lacustris* for astaxanthin production retains several limitations due to high cost of cultivation technique, and its low cell concentration and slow growth (specific growth rate of 0.31/d) [18,19]. Therefore, great efforts have been made to search for more candidates as new astaxanthin producers.

In recent years, yeast has received increasing attention as a substitute source of astaxanthin due to its high biomass productivity (up to 56.4 g/L d) and short cultivation time (3–4 d) compared to microalgae (which require more than 10 d for cultivation and have biomass productivity of about 0.028–0.7 g/L d) [20–22]. In addition, the use of yeast for astaxanthin production eliminates the negative impact of the chemical process on the environment. Particularly, *Rhodosporidium toruloides* (current name: *Rhodotorula toruloides*), an oleaginous yeast (Fungi, Basidiomycota), has been reported as a promising source of carotenoids [23,24]. This yeast can use various low-cost carbon sources and grow to very high density (100 g/L dry cell mass) [25]. Recently, our previous study has shown a potential use of *R. toruloides* to facilitate a low-cost approach for astaxanthin production [2]. *R. toruloides* can reach high biomass yield within a short cultivation time (6.84 g/L dry cell mass within four-day cultivation). However, the wild strains of *R. toruloides* have low astaxanthin yield (927.11 µg/L) [2], thus limiting its industrial application. Therefore, increasing efficiency of astaxanthin production by *R. toruloides* can greatly expand the utilization of *R. toruloides*.

The astaxanthin accumulation in microorganisms is generally facilitated in response to the stress conditions such as salinity, nutrients-starvation, pH, temperature, or unfavorable light [26]. Studies have reported that astaxanthin synthesis by microorganisms can also be enhanced by mutagenization [26,27]. Different approaches, including chemical mutagenesis and physical mutagenesis methods, have been developed to generate mutant strains of microorganisms with higher astaxanthin content [26–28]. Among these approaches, the physically treated methods (ultraviolet (UV) and gamma-ray) have been successfully used as a random mutagenesis strategy to generate genetic mutants with higher astaxanthin accumulation in yeasts [29] and algae [26]. In addition, the physical mutagenesis methods are simple, compared to the chemical mutagenesis methods [26]. Therefore, this study proposed, for the first time, the use of *R. toruloides* mutants for enhanced astaxanthin production.

In this work, UV light and gamma irradiation were used as a mutagenesis agent to produce *R. toruloides* mutants. The *R. toruloides* mutants were screened to obtain astaxanthin-overproducing strains. Response surface methodology (RSM) was then employed to optimize the medium compositions for the cultivation of the selected *R. toruloides* mutant to obtain the maximum astaxanthin yield.

2. Materials and Methods

2.1. Yeast Strains and Culture Conditions

Wide-type *R. toruloides* was provided by University of Science, Vietnam National University Ho Chi Minh City, Vietnam. *R. toruloides* strain was grown in the Hansen broth medium (pH 6) containing 10 g/L peptone, 50 g/L sucrose, 3 g/L KH_2PO_4, and 3 g/L $MgSO_4$. The seed culture was

prepared by inoculating *R. toruloides* cells (5%, v/v) into 250-mL Erlenmeyer flasks containing 100 mL of the Hansen broth and incubated at 30 °C with shaking at 200 rpm for 96 h. The prepared cultures were then used for next studies. In all experiments, the flasks and media were sterilized at 121 °C for 20 min.

2.2. Random UV Mutagenesis

The wild-type *R. toruloides* cells cultivated in the Hansen broth medium in the logarithmic phase (cell density of 10^8 cells/mL) were used for UV mutagenesis as described previously [26]. The cells were obtained from the culture by centrifugation at 13,000× *g* rpm for 10 s. The cell pellets were then rinsed twice with distilled water before being resuspended in distilled water to 10^8 cells/mL. The cell suspension (1 mL) was then illuminated at room temperature for different exposure times (5–30 s) using 248 nm UV Display lamp (Mini UV sterilisation cabinet, Cleaver scientific, England). The treated cells (100 µL) were spread on Hansen agar plate and incubated at 30 °C for 7 d in the dark. The survival rates of the UV-treated cells were subsequently determined by counting the colonies on agar plates. The UV-induced mutants were selected and cultivated in the Hansen broth medium for 4 d at 30 °C with shaking to determine the biomass and astaxanthin yield.

2.3. Random Gamma Irradiation Mutagenesis

The wild-type *R. toruloides* cultivated in the Hansen broth medium in the logarithmic phase (cell density of 10^8 cells/mL) were used for ^{60}Co-gamma mutagenesis as described previously [30]. The cells were obtained from the culture by centrifugation at 13,000× *g* rpm for 10 s. The cell pellets were then rinsed twice with distilled water before being resuspended in distilled water to 10^8 cells/mL. The cell suspension (1 mL) was then irradiated using a ^{60}Co-gamma ray irradiator (GC-5000, India) as a source with 0.5, 1.0, 1.5, 2.0, 2.4, and 3.0 kGy doses. The irradiated cells (100 µL) were plated on Hansen agar medium and incubated at 30 °C for 7 d in the dark. The survival rates of the gamma-treated cells were then determined by counting the colonies on agar plates. The gamma-induced mutants were selected for further cultivation in the Hansen broth medium at 30 °C with shaking for 4 d. The culture was subsequently obtained for biomass and astaxanthin yield determination.

2.4. Optimization of Medium Compositions

The influences of medium compositions on the astaxanthin production by *R. toruloides* mutant were studied using a five-level and three-factorial central composite design. Table 1 illustrates the coded and actual values of the input variables (nutritional parameters). *R. toruloides* mutant were cultivated in the medium containing various peptone concentrations (11.6–28.4 g/L), malt extract concentrations (6.6–23.4 g/L), and glucose concentrations (11.6–28.4 g/L) at 30 °C for 4 d with shaking at 200 rpm. The cells were then collected from the culture to determine the astaxanthin yield. The relation of the determined astaxanthin yield (measured response) to the nutritional parameters was expressed as follows:

$$Y = \beta_0 + \beta_1 X_1 + \beta_2 X_2 + \beta_3 X_3 + \beta_{11} X_1^2 + \beta_{22} X_2^2 + \beta_{33} X_3^2 + \beta_{12} X_1 X_2 + \beta_{13} X_1 X_3 + \beta_{23} X_2 X_3 \quad (1)$$

where Y is the astaxanthin yield (µg/L); X_1 is the peptone concentration (g/L); X_2 is the malt extract concentration (g/L); X_3 is the glucose concentration (g/L); β_0 is the intercept coefficient; β_1–β_3 are the linear coefficients; β_{11}, β_{22}, and β_{33} are the quadratic coefficients; and β_{12}, β_{13}, and β_{23} are the interaction coefficients. These model coefficients were determined using the least-squares method [31]. The experimental design, an analysis of variance (ANOVA), and regression analysis were also conducted using Minitab 16 (Minitab Inc., State College, PA, USA). The established model was subsequently applied to examine the combined effect of the input variables and determine the optimal medium compositions for maximizing astaxanthin yield by solving the regression equation [31].

Table 1. Coded values of the variables for the central composite design.

Variables	Symbols	Levels				
		−1.68 (−α)	**−1**	**0**	**1**	**1.68 (+α)**
Peptone concentration (g/L)	X_1	11.6	15	20	25	28.4
Malt extract concentration (g/L)	X_2	6.6	10	15	20	23.4
Glucose concentration (g/L)	X_3	11.6	15	20	25	28.4

2.5. Analysis

2.5.1. Determination of Survival Rate

The survival rate of *R. toruloides* cells was calculated as follows [8]:

$$Survival\ rate\ (\%) = \frac{C_s}{C_c} \times 100 \quad (2)$$

where C_S and C_c are the total colony count after treatment (by UV or gamma irradiation) and the control (sample without treatment), respectively.

2.5.2. Biomass Determination

The yeast cells were obtained from the culture by centrifugation at 4000× *g* rpm for 5 min. The cell pellets were subsequently rinsed twice with distilled water and dried at 60 °C to a constant weight. Yeast biomass was calculated and expressed as grams in dry weight per liter of culture medium (g/L). The dried biomass was then used to determine astaxanthin content.

2.5.3. Astaxanthin Content Determination

Astaxanthin content was determined based on the methods of Fang and Cheng [32] and An et al. [33] with modifications. Dried biomass (0.2 g) was ground in 3 mL dimethyl sulfoxide (DMSO) in a glass homogenizer for 30 min. The mixture was centrifuged at 4000× *g* rpm for 5 min to obtain the supernatant. The pellet containing residual pigments was well mixed with acetone (5 mL) and centrifuged at 4000× *g* rpm for 5 min to obtain the supernatant. This acetone-extraction step was repeatedly performed 2–3 times to extract all pigment from the solid residue. The DMSO and acetone extracts were then mixed with petroleum ether (1:2, v/v), 10 mL of distilled water, and 5 mL of 20% NaCl solution and placed at room temperature for phase separation. The upper layer containing distilled water, DMSO, and acetone was then removed to obtain the petroleum ether extract. The extract was measured the absorbance at 468 nm against the blank (petroleum ether) using a Genesis 10S UV-Vis spectrophotometer (Thermo Fisher Scientific, Waltham, MA, USA). Astaxanthin content was subsequently calculated as follows [34]:

$$\text{Astaxanthin content}\ (\mu g/g) = \frac{A_{468} \times V \times 10^4}{E_{1\ cm}\% \times G} \quad (3)$$

$$\text{Astaxanthin yield}\ (\mu g/L) = \frac{\text{Astaxanthin content}\ (\mu g/g) \times G}{\text{Volume of culture}\ (L)} \quad (4)$$

where A_{468} is the absorbance of sample at 468 nm; G is the total dry weight of yeast biomass (g); V is the total volume of petroleum ether extract (mL); E_{1cm}% is the absorbance of 1% (w/v) astaxanthin solution in petroleum ether (cuvette width of 1 cm, E_{1cm}% = 2100).

2.5.4. Statistical Analysis

Data were determined in triplicate and shown as the mean ± standard deviation (SD). The data analysis was performed by an ANOVA with the Duncan's multiple range test at p values ≤ 0.05 using SAS software ver 8.2 (SAS Institute, Cary, NC, USA).

3. Results and Discussion

3.1. Astaxanthin Production by UV-Induced Mutants

In this study, the wild-type *R. toruloides* was mutated by using UV and screened for astaxanthin overproducers. After being treated with UV for different exposure times (0–30 s) and cultivated on the solid medium for 7 d, the *R. toruloides* cells were efficiently induced with a rapid color change from slightly pink to red and orange, indicating that UV acts as an inducer for carotenogenesis in *R. toruloides*. The color change in the yeast cells may be due to the respiratory effect of UV light that induces the formation of reactive oxygen species (ROS)-sensitive mutant [35]. Under the UV treatment, the survival of *R. toruloides* cells was declined but the astaxanthin production was significantly promoted. As shown in Figure 1, the survival rate of the *R. toruloides* was dramatically decreased to below 7% with the treatment of UV for longer than 25 s. Although a long UV treatment time caused a low survival rate, it resulted in higher astaxanthin accumulation in the cells. The enhanced astaxanthin production may be due to several protective mechanisms. The carotenoid synthesis in yeast is a complex process, which could be regulated at multiple levels, involving the flow of metabolic intermediates among different pathways, the concentration of carotenogenic gene mRNAs, and the amount of the carotenogenic proteins and their enzymatic activities [36]. When the cells are exposed to oxidative stress (such as UV radiation and gamma irradiation), reactive oxygen species (such as H_2O_2 and $^1O_2$) are produced at the cellular level and cause DNA damage and oxidized proteins [29,35]. To resist the stress, carotenogenesis, which is a photoprotection mechanism in yeast, is subsequently activated to produce carotenoids [35,37]. The produced carotenoids protect the cells by removal of ROS generated by light stress [37]. Studies have reported the presence of singlet oxygen ($^1O_2$) induces the synthesis of astaxanthin by activating enzymes involved in carotenoid biosynthesis [35,38]. Consequently, the UV-induced mutant cells enhanced their astaxanthin production. In addition, mutagenesis process may occur and causes the changes in the nucleotide sequence of several genes (required for carotenoid biosynthesis) to enhance the biosynthesis of astaxanthin [36]. Studies have reported the increase in the mRNA levels of two genes involved in the astaxanthin biosynthesis in yeast, thus enhancing the astaxanthin production [36,39]. For further biomass and astaxanthin analysis, more than 150 mutant cells were selected for cultivation to screen astaxanthin overproducer. Among 150 mutants, 16 strains were proved as the real astaxanthin-overproducer (Table 2). Those strains exhibited a significantly higher astaxanthin yield than the wild-type strain (365.63 μg/L ± 0.42 μg/L). Among the improved mutant strains, the UV6 strain exhibited the highest biomass (4.629 g/L ± 0.0004 g/L) and astaxanthin yield (848.77 μg/L ± 0.77 μg/L). The astaxanthin yield of the UV6 strain was 2.3-fold higher than that of the wild-type strain. This result is comparable to a study reported by Stachowiak [35] that astaxanthin yield was enhanced 1.7-fold by a light-induced mutant strain of *Phaffia rhodozyma* (*Xanthophyllomyces dendrorhous*) 34B compared to the parental strain.

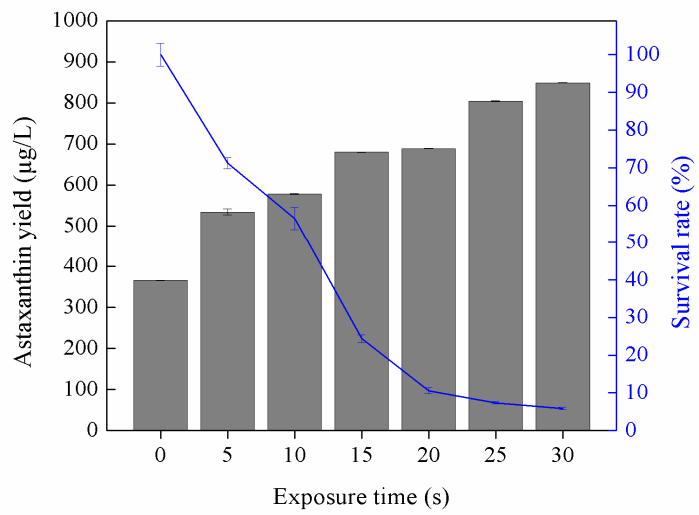

Figure 1. Effect of UV exposure time on the survival rate of wild-type *R. toruloides*. Data are mean ± SD of three replicates.

Table 2. Biomass and astaxanthin production by UV-induced mutants.

Strain	Biomass Yield (g/L)	Astaxanthin Content (μg/g)	Astaxanthin Yield (μg/L)
UV1	2.847 ± 0.0039 ^{dfe}	187.641 ± 0.026 ^{g}	534.28 ± 7.22 ^{j}
UV2	3.461 ± 0.0007 ^{dc}	166.927 ± 0.018 ^{l}	577.68 ± 1.14 ^{h}
UV3	2.684 ± 0.0004 ^{fe}	253.334 ± 0.004 ^{c}	679.95 ± 1.00 ^{e}
UV4	2.931 ± 0.0005 ^{dfe}	194.522 ± 0.003 ^{f}	570.21 ± 0.96 ^{i}
UV5	4.149 ± 0.0004 ^{ab}	144.290 ± 0.002 ^{n}	598.70 ± 0.54 ^{g}
UV6	4.629 ± 0.0004 ^{a}	183.345 ± 0.017 ^{h}	848.77 ± 0.77 ^{a}
UV7	2.931 ± 0.0004 ^{dfe}	274.293 ± 0.002 ^{b}	803.86 ± 1.21 ^{b}
UV8	2.538 ± 0.0002 ^{dfe}	275.241 ± 0.003 ^{a}	698.56 ± 0.55 ^{c}
UV9	3.849 ± 0.0005 ^{bc}	172.380 ± 0.001 ^{j}	663.55 ± 0.87 ^{f}
UV10	1.754 ± 0.0004 ^{g}	232.629 ± 0.007 ^{e}	407.95 ± 1.03 ^{o}
UV11	2.595 ± 0.0003 ^{f}	182.855 ± 0.010 ^{i}	474.51 ± 0.63 ^{m}
UV12	3.016 ± 0.0002 ^{dfe}	171.430 ± 0.002 ^{k}	517.09 ± 0.27 ^{k}
UV13	3.734 ± 0.0002 ^{bc}	130.476 ± 0.007 ^{q}	487.15 ± 0.26 ^{l}
UV14	2.753 ± 0.0003 ^{fe}	250.245 ± 0.003 ^{d}	688.84 ± 0.72 ^{d}
UV15	3.131 ± 0.0003 ^{dfe}	155.485 ± 0.004 ^{m}	486.82 ± 0.40 ^{l}
UV16	3.249 ± 0.0006^{dce}	142.641 ± 0.026 ^{o}	463.49 ± 0.80 ^{n}
WT *	2.777 ± 0.0003 ^{fe}	131.664 ± 0.010 ^{p}	365.63 ± 0.42 ^{p}

* WT: wild-type strain (control). Data are mean ± SD. Means within a column with different letters significantly differ by Duncan's test at $p < 0.05$.

3.2. Astaxanthin Production by Gamma-Induced Mutants

In this work, gamma irradiation was employed as another method to generate *R. toruloides* mutants. The wild-type *R. toruloides* was treated with ^{60}Co-gamma irradiation under different doses and subsequently cultivated on a solid medium for 7 d to screen for astaxanthin overproducers. The *R. toruloides* cells were efficiently induced with a rapid color change from slightly pink to red and orange, indicating that the gamma irradiation induces carotenogenesis in *R. toruloides*. Similar to UV treatment, gamma irradiation treatment also declined survival rates of *R. toruloides*. As shown in Figure 2, the survival rate of the wild-type *R. toruloides* was dramatically decreased with increasing gamma irradiation dose but enhanced the astaxanthin accumulation in the cells. This result indicated that the enhanced astaxanthin production protects the cells against gamma irradiation. Studies have reported that gamma irradiation produces oxygen radicals, which modify the astaxanthin biosynthesis pathway in yeast [29,30]. The oxygen radicals may change enzyme activity or protein properties and may also induce the mutation of yeast through a chromosomal rearrangement [29,30]. Consequently, the mutant strains increase their astaxanthin biosynthesis [29,30]. To screen astaxanthin overproducer,

more than 150 mutant cells were selected for cultivation. Among them, 20 strains were proved as the real astaxanthin-overproducer (Table 3). Those strains showed a significantly higher biomass yield, astaxanthin content, and astaxanthin yield than the wild-type strain. Notably, the gamma-induced mutant strains showed higher astaxanthin accumulation than the UV-induced mutant strains, indicating the gamma irradiation was more efficient than UV treatment to produce astaxanthin-overproducing *R. toruloides* mutants. Among all mutant strains (UV-induced and gamma irradiation-induced mutants), G17 strain exhibited the highest astaxanthin content (603.659 μg/g ± 0.025 μg/g) and astaxanthin yield (1990.26 μg/L ± 1.68 μg/L). The astaxanthin yield of the G17 strain was 5.4-fold higher than that of the wild strain. This result is in agreement with another study that a gamma-induced mutant strain of *P. rhodozyma* YZUXHONG686 exhibited 17-fold higher astaxanthin yield than the parental strain [40]. Therefore, G17 strain was selected for further experiments.

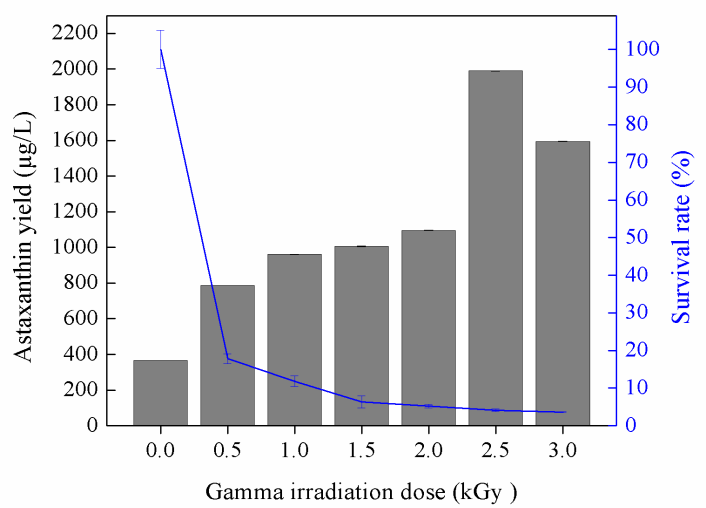

Figure 2. Effect of ^{60}Co-gamma irradiation dose on the survival rate of wild-type *R. toruloides*. Data are mean ± SD of three replicates.

Table 3. Biomass and astaxanthin production by gamma-induced mutants.

Strain	Biomass Yield (g/L)	Astaxanthin Content (μg/g)	Astaxanthin Yield (μg/L)
G1	4.737 ± 0.0007 ^{e}	206.602 ± 0.023 ^{o}	978.67 ± 1.0 ^{j}
G2	3.710 ± 0.0002 ^{l}	212.161 ± 0.030 ^{l}	787.12 ± 0.4 ^{n}
G3	4.556 ± 0.0004 ^{f}	210.909 ± 0.019 ^{m}	960.90 ± 0.6 ^{k}
G4	5.113 ± 0.0015 ^{c}	196.645 ± 0.030 ^{r}	1005.45 ± 2.0 ^{h}
G5	5.403 ± 0.0003 ^{a}	220.475 ± 0.045 ^{i}	1191.23 ± 0.6 ^{c}
G6	3.855 ± 0.0004 ^{k}	229.481 ± 0.035 ^{f}	884.65 ± 0.8 ^{l}
G7	4.236 ± 0.0006 ^{i}	185.002 ± 0.040 ^{s}	783.67 ± 0.9 ^{o}
G8	3.845 ± 0.0004 ^{k}	230.779 ± 0.030 ^{e}	887.34 ± 0.7 ^{l}
G9	4.071 ± 0.0005 ^{j}	218.515 ± 0.025 ^{j}	889.57 ± 0.8 ^{l}
G10	5.104 ± 0.0004 ^{c}	214.647 ± 0.035 ^{k}	1095.56 ± 0.7 ^{f}
G11	5.098 ± 0.0005 ^{c}	228.490 ± 0.010 ^{g}	1164.84 ± 0.7 ^{d}
G12	4.943 ± 0.0004 ^{d}	200.579 ± 0.041 ^{q}	991.46 ± 0.7 ^{i}
G13	4.474 ± 0.0004 ^{h}	233.815 ± 0.050 ^{d}	1046.09 ± 0.9 ^{g}
G14	4.724 ±0.0005 ^{e}	208.408 ± 0.037 ^{n}	984.52 ± 0.8 ^{j}
G15	4.254 ± 0.0005 ^{i}	204.344 ± 0.077 ^{P}	869.28 ± 1.0 ^{m}
G16	4.516 ± 0.0003 ^{g}	253.835 ± 0.025 ^{c}	1146.32 ± 0.5 ^{e}
G17	3.297 ± 0.0408 ^{m}	603.659 ± 0.025 ^{a}	1990.26 ± 1.68 ^{a}
G18	5.245 ± 0.0024 ^{b}	222.142 ± 0.497 ^{h}	1165.14± 6.3 ^{d}
G19	4.729 ± 0.0004 ^{e}	337.306 ± 0.035 ^{b}	1595.12 ± 1.0 ^{b}
G20	4.563 ± 0.0003 ^{f}	173.364 ± 0.040 ^{t}	791.06 ± 0.4 ^{n}
WT *	2.777 ± 0.0003 ^{l}	131.664 ± 0.010 ^{u}	365.63 ± 0.42 ^{p}

* WT: wild-type strain (control). Data are mean ± SD. Means within a column with different letters significantly differ by Duncan's test at $p < 0.05$.

3.3. Optimization of Medium Compositions Using RSM

3.3.1. Development of RSM Model

The nutrients in culture medium are crucial factors affecting the growth and metabolism of microorganisms [2,41]. Studies have reported that astaxanthin accumulation is strongly affected by the medium compositions [2,42]. To maximize the astaxanthin production by the *R. toruloides*, the mutant G17 was cultivated in the medium containing different concentrations of peptone, malt extract, and glucose (Table 4). The relationship between three nutritional parameters (peptone, malt extract, and glucose concentrations) and astaxanthin yield was then evaluated using RSM model to obtain the optimal medium compositions. As can be seen from Table 4, the central experiments (runs 15–20) presented a low coefficient of variance (CV = 0.49%), demonstrating the reproducibility of the experiments. Therefore, the relationship between astaxanthin yield and three nutritional parameters were modeled as follows:

$$Y = 2995.97 - 41.55X_1 - 105.97X_2 - 1.4X_3 - 277.56X_1^2 - 179.39X_2^2 - 246.8X_3^2 - 14.86X_1X_2 + 23.17X_1X_3 + 17.56X_2X_3 \quad (5)$$

where $X_{1\times3}$ and $X_{2\times3}$ have positive influences on the measured response, whereas the other parameters have negative influences.

Table 4. Central composite design matrix for the effect of the nutritional parameters on the astaxanthin yield in coded values and experimental results.

Run	Variables			Response, *Y* (μg/L)	
	X_1	X_2	X_3	Actual Value	Predicted Value
1	−1	−1	−1	2514.50	2467.02
2	−1	−1	1	2425.02	2382.75
3	1	−1	−1	2401.92	2367.29
4	1	−1	1	2451.20	2375.71
5	−1	1	−1	2270.44	2249.67
6	−1	1	1	2297.28	2235.65
7	1	1	−1	2144.48	2090.50
8	1	1	1	2217.93	2169.16
9	0	0	−1.68	2253.40	2300.27
10	0	0	1.68	2206.29	2295.55
11	−1.68	0	0	2224.83	2280.79
12	1.68	0	0	2060.85	2141.02
13	0	−1.68	0	2594.37	2666.81
14	0	1.68	0	2246.67	2310.36
15	0	0	0	3014.95	2995.97
16	0	0	0	2981.78	2995.97
17	0	0	0	3016.95	2995.97
18	0	0	0	2988.78	2995.97
19	0	0	0	3004.95	2995.97
20	0	0	0	2991.78	2995.97

The model (Equation (5)) was then evaluated using F test for ANOVA. As can be seen from Table 5, *p* value of the model was 0.0001, signifying that the established model was statistically significant at the 95% confidence level. Furthermore, the coefficient of determination (R^2) and adjusted R^2 were 0.98 and 0.96, respectively, demonstrating the precision of the model for predicting the astaxanthin yield. The adequate precision was 17.99, which was greater than four, signifying that the signal was adequate, and the developed model could be efficiently used to navigate the design space. As can be seen from Table 4, a good agreement between the actual and predicted values of the astaxanthin concentration was observed; therefore, the developed model could provide reliable results. In addition, the *t* test was used to evaluate the overall influences of the nutritional parameters on the astaxanthin

yield. As shown in Table 6, small p values (<0.05) were observed for the constant, a linear term X_2, and all quadratic terms, indicating that they were crucial parameters in the medium compositions. The established model was subsequently applied to predict the optimal medium compositions for maximizing astaxanthin yield.

Table 5. ANOVA for the empirical model.

Source	DF [b]	SS [b]	MS [b]	F Value	Probability (P) > F
Model [a]	9	2,251,169	250,130	49.39	<0.0001
Residual (error)	10	50,642	5064		
Lack-of-fit	5	49,582	9916	46.75	<0.0001
Total	19	2,301,811			

[a] Coefficient of determination (R^2) = 0.98; adjusted R^2 = 0.96.[b] DF, degree of freedom; SS, sum of squares; MS, mean square. Coefficient of variance (CV) = 0.49%; adequate precision = 17.99.

Table 6. Significance of the coefficients in the empirical model.

Model Term	Parameter Estimate	Standard Error	t Value [a]	p Value
β_0	2995.97	29.02	103.23	0.000 [b]
β_1	−41.55	19.26	−2.16	0.056
β_2	−105.97	19.26	−5.503	0.000 [b]
β_3	−1.40	19.26	−0.07	0.943
β_{11}	−277.56	18.75	−14.81	0.000 [b]
β_{22}	−179.39	18.75	−9.57	0.000 [b]
β_{33}	−246.80	18.75	−13.17	0.000 [b]
β_{12}	−14.86	25.16	−0.59	0.568
β_{13}	23.17	25.16	0.92	0.379
β_{23}	17.56	25.16	0.70	0.501

[a] $t_{\alpha/2,n\text{-}p} = t_{0.025,10} = 2.23$. [b] $p < 0.05$ indicates that the model terms are significant.

3.3.2. Combined Effect of Nutritional Parameters

Figure 3 presents the combined effects of the concentrations of peptone and malt extract on the astaxanthin production while keeping glucose concentration at a central level. At a given malt extract concentration, the astaxanthin yield enhanced with increasing the amount of peptone. This is because peptone supported the biosynthesis of astaxanthin in *R. toruloides* [32]. Nevertheless, a further increase in the peptone amount caused a decline in astaxanthin accumulation. This could be explained that high peptone concentration resulted in a decrease in ratio of carbon to nitrogen, which consequently causes a suppression of the cell growth and the biosynthesis of secondary pigments [43]. Initial ratio of carbon to nitrogen in the medium has reported to significantly influence the astaxanthin synthesis in yeast including *R. toruloides* [2]. A high ratio of carbon to nitrogen suppresses the synthesis of protein, which consequently reduces NADPH consumption for primary metabolism. As a result, more NADPH is available for the astaxanthin synthesis, thus increasing the astaxanthin production [43,44]. This result is similar to the astaxanthin production in microalgae (*C. zofingiensis*) [44] and yeast (*Phaffia rhodozyma*) [45], which requires a high ratio of carbon to nitrogen for the biosynthesis of astaxanthin.

Figure 4 illustrates the combined effects of concentrations of peptone and glucose on the astaxanthin accumulation. At any amount of peptone, astaxanthin yield increased with increasing glucose concentration. This could be explained that glucose enhances metabolism and cell growth [46]. Studies have demonstrated that a sufficient amount of glucose promoted astaxanthin accumulation in yeast through the carotenogenesis pathway [47,48]. During the fermentation, yeast cells use glucose as a substrate to synthesize intermediates such as ethanol and acetic acid. The synthesized ethanol is subsequently converted to acetyl CoA (a precursor for the synthesis of carotenoids) by alcohol dehydrogenase, thus facilitating the biosynthesis of carotenoids [48]. Nevertheless, a higher glucose amount caused a decrease in astaxanthin accumulation. This could be because the cell growth is

suppressed by the excess glucose, and high sugar osmotic pressure induces the production of energetic substances such as protein to resist the environmental stress [46], thus reducing the astaxanthin production. This finding is consistent with the astaxanthin accumulation in *P. rhodozyma* [48] and microalgae *C. zofingiensis* [47].

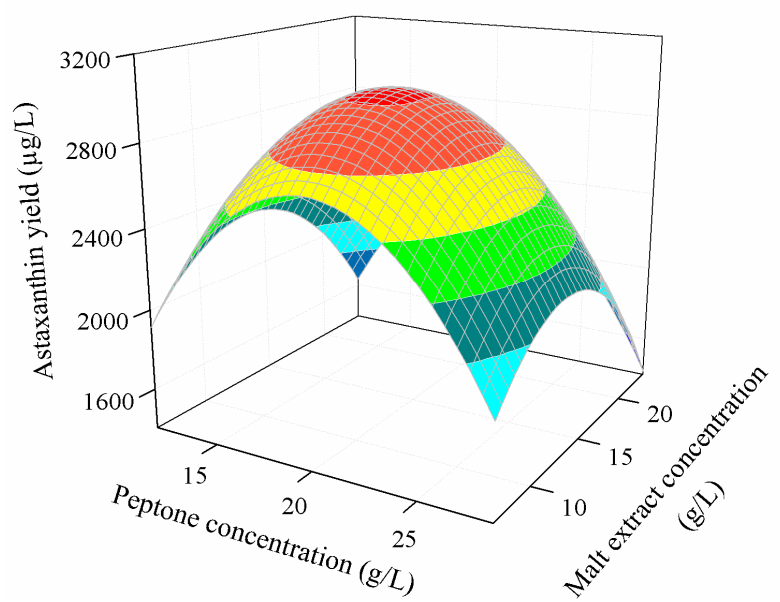

Figure 3. Combined effect of peptone concentration and malt extract concentration on astaxanthin production by *R. toruloides* mutant.

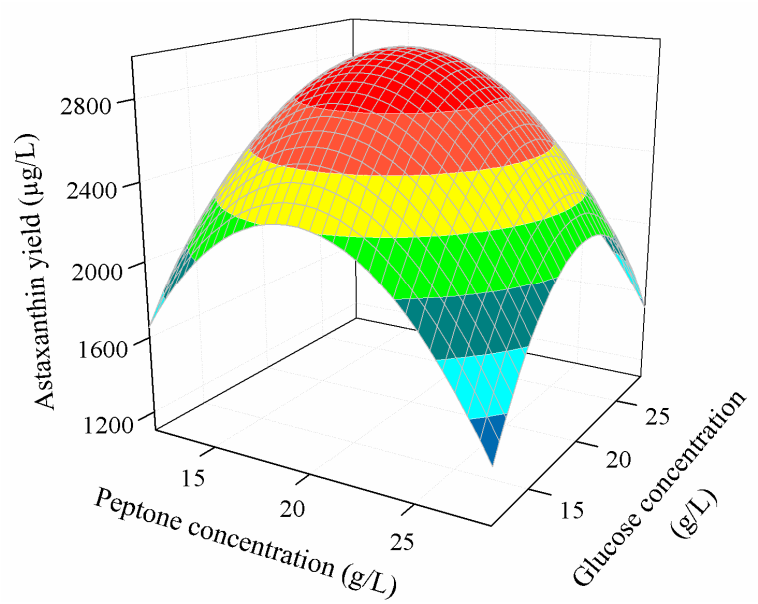

Figure 4. Combined effect of peptone concentration and glucose concentration on astaxanthin production by *R. toruloides* mutant.

Figure 5 presents the combined effect of malt extract and glucose concentrations on the astaxanthin yield when maintaining peptone concentration at a central level. At any glucose concentration, the astaxanthin yield considerably increased with increasing amount of malt extract. This might be because malt extract plays an important role as a complex of nitrogen and carbon source, which promotes the growth of yeast, resulting in higher astaxanthin yield [49–51]. In this work, malt extract was used as an additional nitrogen source for the cultivation of *R. toruloides*. The result showed that malt

extract exhibited a significant effect on astaxanthin synthesis ($p < 0.05$) while peptone had insignificant effect ($p > 0.05$) in the evaluated range (Table 6). Studies have reported that the nitrogen level of malt extract may differ from 1.4% to 1.8% which may be insufficient in itself [49], but when mixed with another nitrogen source (peptone in this study), it was observed to be essential for *R. toruloides* to synthesize astaxanthin. However, a further increase in malt extract resulted in a decline in astaxanthin accumulation due to the negative effect of high levels of nitrogen on the astaxanthin biosynthesis [2].

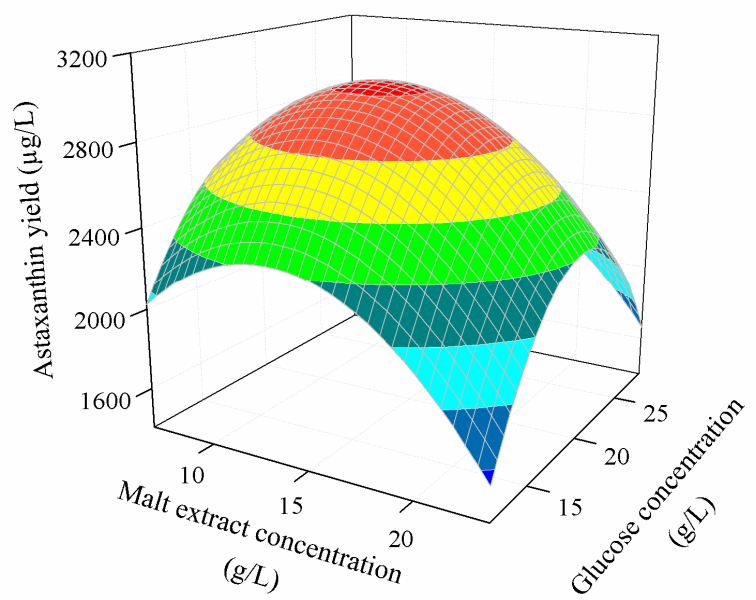

Figure 5. Combined effect of malt extract concentration and glucose concentration on astaxanthin production by *R. toruloides* mutant.

3.3.3. Obtaining Optimal Medium Compositions

By solving the RSM model (Equation (5)), the optimal medium compositions were predicted to be peptone concentration of 19.75 g/L, malt extract concentration of 13.56 g/L, and glucose concentration of 19.92 g/L, with the corresponding astaxanthin yield of 3012.68 µg/L. To verify the prediction, an experiment was performed under the optimized medium compositions. An astaxanthin yield of 3021.34 µg/L ± 16.49 µg/L was obtained, signifying a good agreement with the model prediction. Consequently, the established RSM model can be used to describe the relationship between astaxanthin accumulation and nutritional parameters in the cultivation of *R. toruloides*. *R. toruloides* mutant exhibited a higher astaxanthin yield than *Spirulina platensis* (38 µg/L) [8] and *P. rhodozyma* (639.6 µg/L) [40]. Although the astaxanthin accumulation in *R. toruloides* mutant was lower than that in *Thraustochytrium striatum* (6.2 mg/L) [52] and microalgae *H. lacustris* (84.8 mg/L) [53], the *R. toruloides* is more efficient than these microorganisms in term of fast growth rate and short cultivation time (Table 7). Notably, *R. toruloides* mutant exhibited 3.3-fold higher astaxanthin yield than the wild-type *R. toruloides* (927.1 µg/L) reported in a previous study [2], indicating the gamma irradiation efficiently enhanced the astaxanthin production in *R. toruloides*. Those results suggested that *R. toruloides* mutant could be a promising source for the astaxanthin production. Further studies are still required to enhance the astaxanthin production of *R. toruloides*.

Table 7. Astaxanthin production by several microorganisms.

Strains	Cultivation Time (d)	Astaxanthin Yield (μg/L)	References
Spirulina platensis	10	38	[8]
Phaffia rhodozyma	8	639.6	[40]
Thraustochytrium striatum	15	6200	[52]
Haematococcus lacustris	30	84,800	[53]
R. toruloides (wild strain)	4	927.1	[2]
R. toruloides (mutant)	4	3021.3	This study

4. Conclusions

This paper reports the generation of *R. toruloides* mutants for enhanced astaxanthin production using UV and gamma irradiation mutagenesis. The UV- and gamma-induced mutants exhibited a higher astaxanthin production than that of a wild-type strain. Among the screened mutants, the gamma-induced mutant G17 showed the highest astaxanthin content (603.70 μg/g) and astaxanthin yield (1990.26 μg/L). To further increase the astaxanthin production, the medium compositions for the cultivation of G17 strain were then optimized for maximizing the astaxanthin yield. Through RSM, the optimal medium compositions were determined and a maximum astaxanthin yield of 3021.34 μg/L was obtained. This study suggests that the *R. toruloides* mutant strain of G17 is a potential microbial source for astaxanthin production.

Author Contributions: Conceptualization, T.N.T., H.C.N., and D.-N.N.; methodology, T.N.T. and D.-H.N.; validation, D.-H.N. and Q.T.T; formal analysis, T.N.T. and H.C.N.; investigation, T.N.T., D.-H.N., Q.T.T., and C.-H.S.; resources, D.-N.N.; writing—original draft preparation, H.C.N.; writing—review and editing, H.C.N. and D.-N.N.; supervision, D.-N.N. and H.C.N.; project administration, D.-N.N.; funding acquisition, D.-N.N. All authors have read and agreed to the published version of the manuscript.

Funding: This research was funded by Vietnam National University Ho Chi Minh City, grant number B2019-18-03.

Conflicts of Interest: The authors declare no conflict of interest.

References

1. Batghare, A.H.; Singh, N.; Moholkar, V.S. Investigations in ultrasound–induced enhancement of astaxanthin production by wild strain *Phaffia rhodozyma* MTCC 7536. *Bioresour. Technol.* **2018**, *254*, 166–173. [CrossRef]
2. Tran, T.N.; Quang-Vinh, T.; Huynh, H.T.; Hoang, N.-S.; Nguyen, H.C.; Dai-Nghiep, N. Astaxanthin production by newly isolated *Rhodosporidium toruloides*: Optimization of medium compositions by response surface methodology. *Not. Bot. Horti Agrobo.* **2019**, *47*, 320–327. [CrossRef]
3. Ambati, R.R.; Phang, S.-M.; Ravi, S.; Aswathanarayana, R.G. Astaxanthin: Sources, extraction, stability, biological activities and its commercial applications—A review. *Mar. Drugs* **2014**, *12*, 128–152. [CrossRef]
4. Wu, Y.; Yan, P.; Liu, X.; Wang, Z.; Tang, Y.-J.; Chen, T.; Zhao, X. Combinatorial expression of different β-carotene hydroxylases and ketolases in *Escherichia coli* for increased astaxanthin production. *J. Ind. Microbiol. Biotechnol.* **2019**, *46*, 1505–1516. [CrossRef]
5. Jiang, W.; Zhao, H.; Zhang, L.; Wu, B.; Zha, Z. Maintenance of mitochondrial function by astaxanthin protects against bisphenol A-induced kidney toxicity in rats. *Biomed. Pharmacother.* **2020**, *121*, 109629. [CrossRef]
6. Davinelli, S.; Nielsen, M.E.; Scapagnini, G. Astaxanthin in skin health, repair, and disease: A comprehensive review. *Nutrients* **2018**, *10*, 522. [CrossRef]
7. Panis, G.; Carreon, J.R. Commercial astaxanthin production derived by green alga *Haematococcus pluvialis*: A microalgae process model and a techno-economic assessment all through production line. *Algal Res.* **2016**, *18*, 175–190. [CrossRef]
8. An, J.; Gao, F.; Ma, Q.; Xiang, Y.; Ren, D.; Lu, J. Screening for enhanced astaxanthin accumulation among *Spirulina platensis* mutants generated by atmospheric and room temperature plasmas. *Algal Res.* **2017**, *25*, 464–472. [CrossRef]
9. Dong, H.; Li, X.; Xue, C.; Mao, X. Astaxanthin preparation by fermentation of esters from *Haematococcus pluvialis* algal extracts with *Stenotrophomonas* species. *Biotechnol. Prog.* **2016**, *32*, 649–656. [CrossRef] [PubMed]

10. Liu, Y.; Cui, Y.; Chen, J.; Qin, S.; Chen, G. Metabolic engineering of *Synechocystis* sp. PCC6803 to produce astaxanthin. *Algal Res.* **2019**, *44*, 101679. [CrossRef]
11. Choi, Y.-E.; Yun, Y.S.; Park, J. Evaluation of factors promoting astaxanthin production by a unicellular green alga, *Haematococcus pluvialis*, with fractional factorial design. *Biotechnol. Prog.* **2002**, *18*, 1170–1175. [CrossRef] [PubMed]
12. Guyomarc'h, F.; Binet, A.; Dufossé, L. Production of carotenoids by *Brevibacterium linens*: Variation among strains, kinetic aspects and HPLC profiles. *J. Ind. Microbiol. Biotechnol.* **2000**, *24*, 64–70. [CrossRef]
13. Zhang, C.; Seow, V.Y.; Chen, X.; Too, H.-P. Multidimensional heuristic process for high-yield production of astaxanthin and fragrance molecules in *Escherichia coli*. *Nat. Commun.* **2018**, *9*, 1–12. [CrossRef] [PubMed]
14. Zhang, Z.; Huang, J.J.; Sun, D.; Lee, Y.; Chen, F. Two-step cultivation for production of astaxanthin in *Chlorella zofingiensis* using a patented energy-free rotating floating photobioreactor (RFP). *Bioresour. Technol.* **2017**, *224*, 515–522. [CrossRef] [PubMed]
15. Azizi, M.; Hejazi, M.A.; Hashemi, M. Supplementation with polyalcohols and sequential mixotrophy dilution photoinduction strategy boost the accumulation of astaxanthin by *Haematococcus pluvialis*. *Aquaculture* **2019**, *511*, 734225. [CrossRef]
16. Liu, Y.-H.; Alimujiang, A.; Wang, X.; Luo, S.-W.; Balamurugan, S.; Yang, W.-D.; Liu, J.-S.; Zhang, L.; Li, H.-Y. Ethanol induced jasmonate pathway promotes astaxanthin hyperaccumulation in *Haematococcus pluvialis*. *Bioresour. Technol.* **2019**, *289*, 121720. [CrossRef]
17. Christian, D.; Zhang, J.; Sawdon, A.J.; Peng, C.-A. Enhanced astaxanthin accumulation in *Haematococcus pluvialis* using high carbon dioxide concentration and light illumination. *Bioresour. Technol.* **2018**, *256*, 548–551. [CrossRef]
18. Kaewpintong, K.; Shotipruk, A.; Powtongsook, S.; Pavasant, P. Photoautotrophic high-density cultivation of vegetative cells of *Haematococcus pluvialis* in airlift bioreactor. *Bioresour. Technol.* **2007**, *98*, 288–295. [CrossRef]
19. Li, J.; Zhu, D.; Niu, J.; Shen, S.; Wang, G. An economic assessment of astaxanthin production by large scale cultivation of *Haematococcus pluvialis*. *Biotechnol. Adv.* **2011**, *29*, 568–574. [CrossRef]
20. Dias, C.; Sousa, S.; Caldeira, J.; Reis, A.; da Silva, T.L. New dual-stage pH control fed-batch cultivation strategy for the improvement of lipids and carotenoids production by the red yeast *Rhodosporidium toruloides* NCYC 921. *Bioresour. Technol.* **2015**, *189*, 309–318. [CrossRef]
21. Wu, Y.-H.; Yang, J.; Hu, H.-Y.; Yu, Y. Lipid-rich microalgal biomass production and nutrient removal by *Haematococcus pluvialis* in domestic secondary effluent. *Ecol. Eng.* **2013**, *60*, 155–159. [CrossRef]
22. García-Malea, M.C.; Acién, F.G.; Del Río, E.; Fernández, J.M.; Cerón, M.C.; Guerrero, M.G.; Molina-Grima, E. Production of astaxanthin by *Haematococcus pluvialis*: Taking the one-step system outdoors. *Biotechnol. Bioeng.* **2009**, *102*, 651–657. [CrossRef] [PubMed]
23. González-García, Y.; Rábago-Panduro, L.M.; French, T.; Camacho-Córdova, D.I.; Gutiérrez-González, P.; Córdova, J. High lipids accumulation in *Rhodosporidium toruloides* by applying single and multiple nutrients limitation in a simple chemically defined medium. *Ann. Microbiol.* **2017**, *67*, 519–527. [CrossRef]
24. Zhang, C.; Shen, H.; Zhang, X.; Yu, X.; Wang, H.; Xiao, S.; Wang, J.; Zhao, Z.K. Combined mutagenesis of *Rhodosporidium toruloides* for improved production of carotenoids and lipids. *Biotechnol. Lett.* **2016**, *38*, 1733–1738. [CrossRef] [PubMed]
25. Yaegashi, J.; Kirby, J.; Ito, M.; Sun, J.; Dutta, T.; Mirsiaghi, M.; Sundstrom, E.R.; Rodriguez, A.; Baidoo, E.; Tanjore, D. *Rhodosporidium toruloides*: A new platform organism for conversion of lignocellulose into terpene biofuels and bioproducts. *Biotechnol. Biofuels* **2017**, *10*, 241. [CrossRef] [PubMed]
26. Hong, M.E.; Choi, H.I.; Kwak, H.S.; Hwang, S.-W.; Sung, Y.J.; Chang, W.S.; Sim, S.J. Rapid selection of astaxanthin-hyperproducing *Haematococcus* mutant via azide-based colorimetric assay combined with oil-based astaxanthin extraction. *Bioresour. Technol.* **2018**, *267*, 175–181. [CrossRef]
27. Ang, F.; Khaw, S.; Few, L.; Too, W.S.; Chew, A. Isolation of a stable astaxanthin-hyperproducing mutant of *Xanthophyllomyces dendrorhous* through random mutagenesis. *Appl. Biochem. Microbiol.* **2019**, *55*, 255–263. [CrossRef]
28. Wang, N.; Guan, B.; Kong, Q.; Sun, H.; Geng, Z.; Duan, L. Enhancement of astaxanthin production from *Haematococcus pluvialis* mutants by three-stage mutagenesis breeding. *J. Biotechnol.* **2016**, *236*, 71–77. [CrossRef]

29. Najafi, N.; Ahmadi, A.-R.; Hosseini, R.; Golkhoo, S. Gamma irradiation as a useful tool for the isolation of astaxanthin-overproducing mutant strains of *Phaffia rhodozyma*. *Can. J. Microbiol.* **2011**, *57*, 730–734. [CrossRef]
30. Sun, N.; Lee, S.; Song, K.B. Characterization of a carotenoid-hyperproducing yeast mutant isolated by low-dose gamma irradiation. *Int. J. Food Microbiol.* **2004**, *94*, 263–267. [CrossRef]
31. Su, C.H.; Nguyen, H.C.; Nguyen, M.L.; Tran, P.T.; Wang, F.M.; Guan, Y.L. Liquid lipase-catalyzed hydrolysis of gac oil for fatty acid production: Optimization using response surface methodology. *Biotechnol. Prog.* **2018**, *34*, 1129–1136. [CrossRef] [PubMed]
32. Fang, T.J.; Cheng, Y.-S. Improvement of astaxanthin production by *Phaffia rhodozyma* through mutation and optimization of culture conditions. *J. Ferment. Bioeng.* **1993**, *75*, 466–469. [CrossRef]
33. An, G.-H.; Bielich, J.; Auerbach, R.; Johnson, E.A. Isolation and characterization of carotenoid hyperproducing mutants of yeast by flow cytometry and cell sorting. *Biotechnology* **1991**, *9*, 70–73. [CrossRef] [PubMed]
34. Kelley, C.E.; Harmon, A.W. Method of determining carotenoid contents of Alaska pink shrimp and representative values for several shrimp products. *Fish. Bull.* **1972**, *70*, 111.
35. Stachowiak, B. Effect of illumination intensities on astaxanthin synthesis by *Xanthophyllomyces dendrorhous* and its mutants. *Food Sci. Biotechnol.* **2013**, *22*, 1033–1038. [CrossRef]
36. Castelblanco-Matiz, L.M.; Barbachano-Torres, A.; Ponce-Noyola, T.; Ramos-Valdivia, A.C.; García-Rojas, C.M.C.; Flores-Ortiz, C.M.; Barahona-Crisóstomo, S.K.; Baeza-Cancino, M.E.; Alcaíno-Gorman, J.; Cifuentes-Guzmán, V.H. Carotenoid production and gene expression in an astaxanthin-overproducing *Xanthophyllomyces dendrorhous* mutant strain. *Arch. Microbiol.* **2015**, *197*, 1129–1139. [CrossRef]
37. Vázquez, M. Effect of the light on carotenoid profiles of *Xanthophyllomyces dendrorhous* strains (formerly *Phaffia rhodozyma*). *Food Technol. Biotechnol.* **2001**, *39*, 123–128.
38. Stachowiak, B. Astaxanthin synthesis by *Xanthophyllomyces dendrorhous* DSM 5626 and its mutants on carrot extract medium under different illumination intensity. *Appl. Biochem. Microbiol.* **2014**, *50*, 471–476. [CrossRef]
39. Marcoleta, A.; Niklitschek, M.; Wozniak, A.; Lozano, C.; Alcaíno, J.; Baeza, M.; Cifuentes, V. Glucose and ethanol-dependent transcriptional regulation of the astaxanthin biosynthesis pathway in *Xanthophyllomyces dendrorhous*. *BMC Microbiol.* **2011**, *11*, 190. [CrossRef]
40. Xie, H.; Zhou, Y.; Hu, J.; Chen, Y.; Liang, J. Production of astaxanthin by a mutant strain of *Phaffia rhodozyma* and optimization of culture conditions using response surface methodology. *Ann. Microbiol.* **2014**, *64*, 1473–1481. [CrossRef]
41. Nahidian, B.; Ghanati, F.; Shahbazi, M.; Soltani, N. Effect of nutrients on the growth and physiological features of newly isolated *Haematococcus pluvialis* TMU1. *Bioresour. Technol.* **2018**, *255*, 229–237. [CrossRef] [PubMed]
42. Zhao, Y.; Yue, C.; Geng, S.; Ning, D.; Ma, T.; Yu, X. Role of media composition in biomass and astaxanthin production of *Haematococcus pluvialis* under two-stage cultivation. *Bioprocess Biosys. Eng.* **2019**, *42*, 593–602. [CrossRef] [PubMed]
43. Saenge, C.; Cheirsilp, B.; Suksaroge, T.T.; Bourtoom, T. Potential use of oleaginous red yeast *Rhodotorula glutinis* for the bioconversion of crude glycerol from biodiesel plant to lipids and carotenoids. *Process Biochem.* **2011**, *46*, 210–218. [CrossRef]
44. Ip, P.-F.; Chen, F. Production of astaxanthin by the green microalga *Chlorella zofingiensis* in the dark. *Process Biochem.* **2005**, *40*, 733–738. [CrossRef]
45. Stoklosa, R.J.; Johnston, D.B.; Nghiem, N.P. Utilization of sweet sorghum juice for the production of astaxanthin as a biorefinery co-product by *Phaffia rhodozyma*. *ACS Sustain. Chem. Eng.* **2018**, *6*, 3124–3134. [CrossRef]
46. Nguyen, H.C.; Su, C.-H.; Yu, Y.-K.; Huong, D.T.M. Sugarcane bagasse as a novel carbon source for heterotrophic cultivation of oleaginous microalga *Schizochytrium* sp. *Ind. Crops Prod.* **2018**, *121*, 99–105. [CrossRef]
47. Ip, P.-F.; Wong, K.-H.; Chen, F. Enhanced production of astaxanthin by the green microalga *Chlorella zofingiensis* in mixotrophic culture. *Process Biochem.* **2004**, *39*, 1761–1766. [CrossRef]
48. Fang, T.J.; Wang, J.-M. Extractability of astaxanthin in a mixed culture of a carotenoid over-producing mutant of Xanthophyllomyces dendrorhous and *Bacillus circulans* in two-stage batch fermentation. *Process Biochem.* **2002**, *37*, 1235–1245. [CrossRef]

49. Hossain, T.; Miah, A.B.; Mahmud, S.A. Enhanced bioethanol production from potato peel waste via consolidated bioprocessing with statistically optimized medium. *Appl. Biochem. Biotechnol.* **2018**, *186*, 425–442. [CrossRef]
50. Awad, G.E.; Amer, H.; El-Gammal, E.W.; Helmy, W.A.; Esawy, M.A.; Elnashar, M.M. Production optimization of invertase by *Lactobacillus brevis* Mm-6 and its immobilization on alginate beads. *Carbohydr. Polym.* **2013**, *93*, 740–746. [CrossRef]
51. Tran, N.T.; Pham, D.N.; Kim, C.-J. Production of 5-aminolevulinic acid by recombinant *Streptomyces coelicolor* expressing hemA from *Rhodobacter sphaeroides*. *Biotechnol. Bioprocess Eng.* **2019**, *24*, 488–499. [CrossRef]
52. Xiao, R.; Li, X.; Leonard, E.; Tharayil, N.; Zheng, Y. Investigation on the effects of cultivation conditions, fed-batch operation, and enzymatic hydrolysate of corn stover on the astaxanthin production by *Thraustochytrium striatum*. *Algal Res.* **2019**, *39*, 101475. [CrossRef]
53. Hwang, S.-W.; Choi, H.I.; Sim, S.J. Acidic cultivation of *Haematococcus pluvialis* for improved astaxanthin production in the presence of a lethal fungus. *Bioresour. Technol.* **2019**, *278*, 138–144. [CrossRef] [PubMed]